Signal transmission between gap-junctionally coupled passive cables occurs at an optimal cable diameter

Farzan Nadim
Mathematical Sciences
New Jersey Institute of Technology
973-353-1541, farzan@njit.edu

Jorge Golowasch
Mathematical Sciences
New Jersey Institute of Technology
973-353-1267, jorge.p.golowasch@njit.edu

CAMS Report 0405-36, Fall 2004/Spring 2005
Center for Applied Mathematics and Statistics

Abstract

Theoretical studies have shown that gap junctional coupling can lead to complex network activity. We examine the consequences of current flow between two passive cables coupled by gap junctions at one end and derive analytical solutions for the steady state case. This architecture could represent gap-junctionally coupled processes of two neurons or coupling between two muscle fibers. We find that the transfer of electrical signals across the gap junction between two coupled cables does not always increase with increased cable diameter as expected from the increase in length constants, but that an optimal diameter exists. The optimal cable diameter arises because the gap junction acts as a current limiter. As current flows from one cable to the second, voltage attenuation along the latter follows two opposing rules. At low diameters, voltage attenuation along cable 2 decreases with increasing diameter, while at high diameters, it increases. This is due to an increase in leak conductance in cable 2 and the limited current flow through the gap junction. This optimal diameter depends on the gap junction resistance as well as the membrane properties and lengths of the cables. Moreover, in branched cables dependence on diameter is local and thus may serve to functionally compartmentalize branches that are independently coupled to other cells. Such compartmentalization may be important when periodic signals or action potentials cause the current flow across gap junctions. We predict that, in biological networks, coupled processes may have optimal diameters that maximize signal transfer between cells.

Introduction

Gap junctions are involved in transfer of ions and small molecules between cells in many tissues. Electrical signaling via gap junctions has been implicated in the generation of synchronous electrical activity (1, 2). A number of recent publications have reported the presence of gap junctional coupling between many neuronal types which had not previously been observed (3). These observations highlight the growing importance attributed to gap junctions in the computations performed by many regions of the nervous system. The role of gap junctions in the generation and failure of neuronal oscillations and synchrony has been the subject of many theoretical studies (4-8). However, the relationship between gap junctional strength and the membrane properties of the connecting cells is less well understood (but see (9) for a physiological approach).

We have previously shown that gap junctional coupling can affect the measurements of ionic conductances and that these effects are sensitive to the location and strength of the gap junction (10). The results of this study implied that electrical signaling between neurons becomes more effective if the gap junctional coupling strengthens or if the neurons become more electrotonically compact. Here we report that this intuition is not entirely correct. We observe a non-monotonic dependence of signal transfer between coupled passive cables as a function of cable diameter. Although electrotonic access to a coupled cell improves with increased diameter, signal transfer may not. Our results show that signal transfer is maximized at an optimal cable diameter that depends on the coupling conductance as well as on the cable properties. Thus, signal transfer actually deteriorates as the coupled cables become more electrotonically compact past a certain optimal diameter. The optimal diameter depends on the specific properties of individual branches of the postsynaptic cell. Therefore, functional compartmentalization may arise simply as a result of a difference in cable diameters in branches of coupled neuronal processes. We derive analytical expressions for signal transfer at steady state and examine the transient cases numerically.

Methods

Simulations

Each cable is a sealed-end cylinder with length 600 μm divided into 6 compartments of equal length. The membrane potential of compartment j (indexed from 0 to 5) of cable i is v_{i_j}. The two cables are gap-junctionally coupled at their ends, connecting segments 1_5 to 2_0 (diagram in Fig. 1A). Specific properties are: membrane resistivity $R_m = 40$ kΩcm^2, axial resistivity $R_i = 60$ Ωcm and capacitance $C_m = 10^{-6}$ F/cm^2 (11). In all simulations V_{1_0} is voltage clamped to a fixed value. A spiking isopotential neuron was built using standard Hodgkin & Huxley equations (12). Numerical simulations were performed using the XPP software (13).

Analytical solutions

The steady-state equations for the coupled cables are derived from basic cable theory (14). The steady-state voltage V_x (calculated as deviation from v_{rest}) at any distance

x along a uniform cylindrical cable of finite length l and length constant λ can be calculated as

$$V_x = V_0 \frac{\cosh(L-X)+\frac{R_\infty}{R_L}\sinh(L-X)}{\cosh L+\frac{R_\infty}{R_L}\sinh L} \qquad (1)$$

where $L = l / \lambda$, $X = x / \lambda$, R_∞ is the input resistance of an infinitely long cable and R_L is the terminating resistance at $x = l$. To calculate the current flow between the finite cables electrically coupled at the end (X=L) we determine the voltage at the end of cable 1. For a single uncoupled cable, at $x = l$, Eq. 1 simplifies to

$$V_L = \frac{V_0}{\cosh L + \frac{R_\infty}{R_L}\sinh L} \qquad (2)$$

with $\lambda = \sqrt{d \cdot R_m / 4R_i}$ and $R_\infty = (2/\pi)d^{-3/2}\sqrt{R_m R_i}$. Note that the terminating resistance of cable 1 (R_{L1}), when coupled to cable 2, is simply the sum of the gap junction resistance R_c and the input resistance of cable 2 (R_{in2}) at the site of the gap junction. Since cable 2 has a sealed end,

$$R_{in2} = R_{\infty 2}\coth L_2 = \frac{2\sqrt{R_m R_i}}{\pi d_2^{3/2}}\coth(l_2 / \sqrt{\frac{R_m d_2}{R_i 4}}) \qquad (3)$$

Thus, $R_{L1} = R_{in2} + R_c$ which, together with Eq. 2, gives an expression for the voltage at the end of cable 1:

$$V_{1\_L} = \frac{V_0}{\cosh L_1 + \frac{R_{\infty 1}}{R_c + R_{in2}}\sinh L_1} \qquad (4)$$

Note that, in the absence of coupling ($R_c = \infty$), the length constant λ_1 of cable 1 simply increases as the diameter increases and thus, V_{1_L} approaches V_0.

The beginning of the second cable proximal to the gap junction behaves as a node in which the current flowing from cable 1 through the gap junction is equal and opposite to the current flowing through cable 2, i.e. $I_c + I_{2\_0} = 0$. This equation can be expanded to $(V_{2\_0} - V_{1\_L})/R_c + V_{2\_0} / R_{in2} = 0$. Solving for V_{2_0} we get

$$V_{2\_0} = \frac{R_{in2} V_{1\_L}}{R_c + R_{in2}} \qquad (5)$$

Finally, since cable 2 is a finite cable with a sealed end,

$$V_{2\_L} = \frac{V_{2\_0}}{\cosh L_2} \qquad (6)$$

Equations 4-6 can be used to explicitly evaluate the voltages at the ends of both cables. To obtain the cable diameter at which the value of V_{2_L} is maximum (the optimal diameter), we calculated $\partial V_{2\_L} / \partial d$ and found its positive root with the aid of the software Mathematica (Wolfram Research, Champaign, IL).

Results

An optimal diameter exists when two cables are coupled by gap junctions

Using basic equations of cable theory, it can be readily demonstrated that an elongated process becomes more electrotonically compact if its diameter increases. This is a consequence of the fact that the length constant of a uniform cable is proportional to the square root of its diameter. Therefore, the larger the diameter, the larger the length constant λ and the smaller the electrotonic size (length / λ) of the cable. Consequently, if one end of a finite sealed-end cable is voltage clamped (at $V_{1\_0} \neq 0$ mV), the voltage attenuation along the cable is less if the cable diameter is larger and thus the voltage at the distal end of the cable is closer to V_{1_0}.

If, additionally, this cable is coupled at its distal end via gap-junctions to a second cable, there will be a voltage drop across the gap junction but the voltage attenuation continues along the second cable. This is demonstrated using numerical simulations in Fig. 1A by plotting the voltages along two cables, each of length l = 600 μm, coupled at the end with a gap junction of resistance R_c, when V_{1_0} is voltage clamped at 40 mV. The voltage along cable 1 attenuates; there is a sharp voltage drop across the gap junction and the voltage attenuation continues along cable 2. As the coupling resistance R_c is decreased, the voltage drop across the gap junction becomes less pronounced and the two coupled cables resemble a single cable with length = $l_1 + l_2$ (Fig. 1A).

Figure 1B shows the voltages along the two cables as the diameters of both cables are simultaneously varied. The top 6 traces correspond to voltages along cable 1 and the remaining 6 traces to voltages along cable 2 (as indicated in the schematic). The box denotes the values shown in Fig. 1A with $R_c = 10^7$ Ω and d = 1 μm. As expected, we found that when the proximal end of cable 1 was voltage clamped, the voltage attenuation along this cable decreased as its diameter increased. Surprisingly, this was not the case for voltages along cable 2. Although for any fixed diameter there was voltage attenuation along cable 2, as diameter was increased, at any fixed position along cable 2 voltage first increased and then decreased (Fig. 1B, bottom 6 traces). Thus, for each position along cable 2, there was a cable diameter at which the voltage attenuation was minimal (box in Fig. 1B). We refer to this value as the "optimal diameter."

To understand how the optimal diameter emerges, we used analytical expressions for the steady-state voltages along two uniform cables of finite length, coupled at the end with a gap junction (Methods). Figure 2A shows a comparison of the voltages at the proximal and distal ends of cable 2, calculated using the computational model used in Fig. 1 (symbols) and analytical expressions (curves) calculated using Eqs. 5 and 6. This voltage vs. diameter graph shows an optimal diameter for signal transfer across a gap junction which can also be described as a "diameter tuning curve." We will show that the optimal cable diameter depends on the gap junction resistance as well as the membrane properties of both cables.

Using the analytical expressions (Eqs. 4 and 5), we compared the voltages at the two ends of the gap junction (V_{1_L} and V_{2_0}) when the proximal end of cable 1 (V_{1_0}) was voltage clamped (compare dotted and solid curves in Fig. 2B). As expected, V_{1_L} (dotted trace) approached the value of V_{1_0} (= 40 mV) as the cable diameters (d) increased. Within a range of relatively small d values, the voltages across the gap junction were close in value and V_{2_0} (solid trace) tracked V_{1_L}. However, as d increased further, V_{1_L} approached a plateau but V_{2_0} began to decrease.

The rise and fall of V_{2_0} as a function of d can be readily explained using Eqs. 3 and 5. At small d values, the input resistance of cable 2 (R_{in2}) is relatively large. In fact, in this range of d, R_{in2} is much larger than the gap junction resistance R_c and thus, to first approximation, R_c can be ignored in the denominator of Eq. 5 and V_{2_0} tracks V_{1_L}, which is increasing. However, R_{in2} decreases as d increases (Eq. 3) and, for large d, R_{in2} becomes much smaller than R_c. Thus, for large d the value of V_{2_0} decreases with R_{in2} even as the value of V_{1_L} continues to increase and approaches a constant (Eq. 5). In effect, R_c acts as a current limiter: as the diameter of cable 2 increases, it becomes more "leaky" and the R_c-limited current flowing into cable 2 results in a progressively lower current density and more attenuated voltage change along cable 2.

This latter fact can also be demonstrated by voltage clamping cable 1 at its coupled end (V_{1_L}) and plotting V_{2_0} as a function of diameter (Fig. 2B, dashed trace). The value of V_{2_0} is close to V_{1_L} (= 40 mV) for small d but drops as d increases but, in this case, there is no optimal diameter for V_{2_0}. Note however, that the distal portions of cable 2 (e.g., V_{2_L}) still show an optimal diameter (not shown). This is due to the fact that the term $1/\cosh(L_2)$ in Eq. 6 grows monotonically as the diameter of cable 2 increases while V_{2_0} monotonically decreases, independent of the voltage at V_{1_L}. The product of these two terms (Eq. 6) generates the peak voltage at an optimal diameter.

Note that the drop in V_{2_L} is primarily due to the fact that R_{in2} decreases as the diameter of cable 2 increases. Thus, when the diameter changes are restricted only to cable 1 (Fig. 2C, dashed trace) no optimal diameter is observed. However, if only the diameter of cable 2 is modified an optimal diameter does appear (Fig. 2C, dotted trace). This optimal diameter increases when the diameters of both cables are simultaneously modified (Fig. 2C, solid trace) because at low diameters, V_{1_L} is significantly more attenuated compared to V_{1_L} when d_1 is fixed.

Dependence of optimal diameter on membrane properties

The steady-state voltage profile along a cable depends on the specific membrane resistance R_m, specific axial resistance R_i, length and diameter. Figure 3 shows the effects of R_m and R_i on the optimal diameter of two cables coupled with $R_c = 2\times10^8$ Ω. The dependence of optimal diameter on R_m is most pronounced when only R_{m1} is varied (Fig. 3A, solid grey symbols), showing a monotonic exponential decrease as R_{m1} increases and a linear decrease above approximately 10 kΩcm^2. The effect of the R_m of cable 2 on optimal diameter also shows an exponential decrease as R_{m2} increases up to approximately 5 kΩcm^2. At this point, and in contrast to what is seen when R_{m1} is varied,

the optimal diameter starts to increase linearly with R_{m2} (open grey symbols). The combined effect of simultaneously changing R_m in both cables is an exponential decrease as R_m increases up to approximately 10 kΩcm^2 and near-independence of the optimal diameter above this point (black symbols). Although for most of the R_m range the effect on optimal diameter is relatively small (especially when both R_{m1} and R_{m2} are varied simultaneously) there are significant effects on the diameter tuning curve (Fig. 3A inset). As the membrane resistance decreases two things happen: the voltages along cable 2 attenuate and the diameter tuning curve sharpens.

The optimal diameter for signal transfer changes in a monotonic fashion whether R_{i1} or R_{i2} is modified, with the optimal diameter increasing as R_i increases. As in the case of R_m variations, the effect is more pronounced when R_{i1} (Fig. 3B, solid grey symbols) is modified than R_{i2} (open grey symbols). This effect is even more pronounced when R_i in both cables are simultaneously changed (black symbols). The effect of R_i on optimal diameter is somewhat comparable to the effect of R_m in that changes that increase voltage attenuation along either of the two cables (namely by reduction of R_m below 10 kΩcm^2 or increase of R_i) increase the optimal diameter. As in the case of R_m changes, increases in voltage attenuation due to changes in R_i are accompanied by an increased sharpness of the diameter tuning curve (Fig. 3B inset).

Changes in cable length have a similar effect as those changes that increase voltage attenuation (i.e. decreased R_m or increased R_i). Figure 4A shows that increasing the length of cable 1 (solid grey symbols) leads to an almost linear increase in optimal diameter. Increasing the length of cable 2 leads to an initial reduction of optimal diameter at low lengths and then a linear increase for higher values (Fig. 4A, open grey symbols). When both cable lengths are increased simultaneously, the optimal diameter increases monotonically (Fig. 4A, black symbols). This is accompanied by a progressive signal attenuation (not shown). As with changes in R_m or R_i, changes in cable length that lead to the attenuation of voltage result in a sharpening of the diameter tuning curve accompanied by a marked shift in the optimal diameter to larger values (Fig. 4A inset). At the limit when either cable is so short (length = 20 μm) as to be nearly isopotential, an optimal diameter still exists, albeit of different values (Fig. 4B and C). Note that when cable 1 is isopotential, V_{2_0} no longer shows an optimal diameter but the distal points along cable 2 do (Fig. 4B). When cable 2 is isopotential it nonetheless shows an optimal diameter (Fig. 4C).

Dependence of optimal diameter on gap junction resistance

Gap junction resistance sensitively determines optimal diameter for signal transfer between coupled cables. As gap junction resistance increases, the optimal diameter sharply decreases (Fig. 5). Notice that approximately 70% drop occurs between gap junction conductances of 10^6 to 10^7 Ω (Fig. 5). At $R_c = 10^9$ Ω the optimal diameter is reduced by over one order of magnitude compared with $R_c = 10^6$ Ω (Fig. 5), while the amplitude of the signal is attenuated only approximately 50% (not shown). As describe before for the effects of R_m, R_i and length on optimal diameter, attenuation of the signal is accompanied by an increased sharpness in the diameter tuning curve (Fig. 5 inset).

Effect of branching on optimal diameter

The dependence of the optimal diameter on membrane properties suggests that different branches in a dendritic tree, having different membrane properties, may also express different optimal diameters. Indeed, Fig. 6A shows that branches with different membrane resistances but otherwise identical properties display different optimal diameters. When the diameters of both branches are varied simultaneously the cable with lower input resistance (Fig. 6A, grey trace) shows a larger optimal diameter and a sharper but more attenuated diameter tuning curve. This confirms the rule of thumb mentioned before: properties that increase voltage attenuation, increase both the optimal diameter and the sharpness of the diameter tuning curve. This effect is local because diameter changes in a daughter branch produce an optimal diameter only in that branch (Fig. 6B, grey trace). Diameter changes in a mother branch will produce the same optimal diameter in that branch and its daughter branches (Fig. 6C; note that the postsynaptic segment closest to the gap junction is part of the mother branch - see schematic).

Effects of signal frequency on optimal diameter

Although we do not present here the analytical solutions to the transient (non steady-state) case, the behavior of two coupled cables to a sinusoidal change in voltage at the beginning of cable 1 can be intuitively understood in a way similar to the effects of R_m on voltage attenuation and the presence of an optimal diameter for signal transfer along coupled cables. By increasing frequency the impedance of the cables decreases with a consequent increase in signal attenuation (Fig. 7) and, at the same time, the optimal diameter gradually increases (stars and dotted trace) very much like the optimal diameter increases as R_m decreases in both cables simultaneously (Fig. 3A, black trace). The increased signal attenuation at high frequencies is also accompanied by a sharper diameter tuning curve (Fig. 7 inset).

Gap junction-mediated postsynaptic potentials

Recently studies have proposed that axo-axonic gap junctions are present between hippocampal pyramidal neurons and account for the generation of spikelets (15). The results of the current study suggest that transmission of fast action potentials between axons or between axons and other neuronal processes depends on the diameter of the processes involved. To examine this hypothesis, we coupled an action potential-generating single-compartment model neuron to the center of a long cable (Fig. 8, schematic diagram). We found that the postsynaptic potential (PSP) produced by the action potential in the coupled cable shows a maximal amplitude at a unique cable diameter, in this case at approximately 5 μm. The PSP amplitude was diminished if the axon diameter was different. One interesting consequence is that, although the amplitude of the PSP produced at a low diameter (e.g. 1 μm, leftmost inset in Fig. 8) may be almost identical to the amplitude at a diameter higher than the optimal value (e.g. 30 μm, rightmost inset in Fig. 8), the time course of the these PSPs vary greatly owing to the different time constants of the membrane at these different diameters.

Discussion

New experimental results have shown gap junctions to be much more prevalent in the nervous system than previously known. Although the complete functional role of electrical coupling via gap junctions within neuronal networks remains to be revealed, such coupling has been shown to underlie network phenomena such as synchronized activity (3, 16), coincidence detection (17) and pattern generation (18). Few specific pharmacological agents affect gap junctions (3) and direct experimental measurements and manipulations of electrical coupling are notoriously difficult. Consequently, theoretical studies of electrical coupling are necessary to understand the functional consequences of interactions between electrical coupling and the membrane properties of the coupled cells. Surprisingly, few such studies have been carried out (1, 19).

We analyze the effects of interactions between gap junction conductance and cellular properties of coupled cables on signal transfer. We show that two gap-junctionally coupled passive cables will produce maximal signal transfer (electrical PSP) at a certain "optimal" diameter, below or above which signal transfer is diminished. Such optimal diameter can be shown for both steady state signals and for action potentials or periodic signals. This optimal signal transfer may be potentially important in the operation of many systems.

Relationship between gap junctional current flow and voltage changes

We have shown the presence of an optimal diameter when the beginning of cable 1 is voltage clamped. The optimal diameter appears if either both cable diameters or only the diameter of cable 2 are varied (Fig. 2C). However, this optimal diameter disappears if a fixed current is injected into cable 1 and the diameters of both cables are changed simultaneously. Nevertheless, with a fixed current input into cable 1 the optimal diameter still appears if the diameter changes are local to cable 2 only (not shown). Notice that action potentials effectively voltage clamp the membrane. Thus, the occurrence of an action potential in a neuron presynaptic to the gap junction will produce a maximal electrical EPSP for a unique optimal diameter determined by both cables. This is shown in a simplified configuration in Fig. 8. Moreover, for any local subthreshold current input in cable 1 (e.g. a chemical synaptic input) that does not clamp the membrane potential, a maximal signal transfer across the gap junction is determined by the diameter of the second cable only. If both cable diameters are changed simultaneously, for an input of fixed current instead of constant voltage, an optimal diameter does not appear.

An additional effect of the sensitivity of electrical coupling to cable diameter is that, although a signal (e.g. an action potential) may be transmitted with identical attenuation into cables of different diameters, the synaptic integration properties of two otherwise identical cables can be substantially different due to the different membrane properties of a thin and a thick cable (see PSP shape in Fig. 8 at 1 and 30 μm).

Developmental effects

Dendritic pruning during critical stages of development is important in the establishment of functional neural networks and is known to rely on the strengthening of strongly correlated signals between cells (20, 21). Neuronal structure and circuit formation during these critical periods rely on chemical and electrical coupling (20) and dendrite morphology (branching, length, spine density) is regulated by activity (22). Thus, cable diameter may also be an important factor during developmental pruning of gap junctionally coupled dendrites because, as our results show, such coupled processes are likely to be more strongly correlated at diameters close to their optimum for signal transfer. Gap junctionally coupled processes that are most strongly coupled are thus likely to be selected and preserved during pruning. Consequently, it is conceivable that cable diameter, like other morphological neuronal features, may also be regulated during development and thus be another important variable in the determination of network structure and activity.

Network synchronization

Coupling via gap junctions among interneurons has been shown to be important in the generation of synchronous activity in different regions of the mammalian brain (3). These interneuron networks involve co-localized chemical and electrical coupling (2, 23-25) both of which may be involved in producing synchrony (8, 26, 27). We have shown that optimal diameter depends on the membrane resistance of the coupled processes, particularly when this resistance is low (Fig. 3A). Therefore, when chemical synaptic input is low (and thus membrane resistance is high), pairs of neurons could be tuned to be maximally coupled via gap junctions allowing for effective synchronization. Alternatively, synchronization can be driven by chemical synaptic inputs, in which case membrane resistance will be low, bringing the electrical coupling-based signaling out of optimal range. In this way synchrony could be assured via different cellular mechanisms. Moreover, electrical coupling and synaptic inputs can act synergistically to bring about synchrony (2, 8, 25). On the other hand, the removal of chemical synaptic inputs could bring a network to an optimal state for gap junctional signaling by changing R_m and thus induce synchrony. Such a mechanism may be at work where synchrony appears after blocking synaptic transmission (28).

Diameter and gap junction conductance measurements

Optimal signal transfer via gap junctions is a local effect (Fig. 6). Thus, any direct experimental test of such optimal signaling requires measurement of gap junction conductances specific to the coupled processes. Few simultaneous measurements of gap junctional conductance and diameter of the coupled processes have been performed (29). Based on our results, we predict the optimal diameter value for normally observed gap junction conductances and input resistances to be in the sub-micrometer to micrometer range. This appears to be in accordance with observed dendrite diameters where gap junctions have been found and total gap junction conductances estimated (25, 29, 30). We predict that in systems that rely on electrical signaling via gap junctions coupled

processes have diameters that have been selected or regulated to be around an optimal value for maximum signal transfer.

References

1. Perez Velazquez, J. L. & Carlen, P. L. (2000) *Trends Neurosci* **23,** 68-74.
2. Friedman, D. & Strowbridge, B. W. (2003) *J Neurophysiol* **89,** 2601-10.
3. Connors, B. W. & Long, M. A. (2004) *Annu Rev Neurosci* **27,** 393-418.
4. LeBeau, F. E., Traub, R. D., Monyer, H., Whittington, M. A. & Buhl, E. H. (2003) *Brain Res Bull* **62,** 3-13.
5. Traub, R. D., Pais, I., Bibbig, A., LeBeau, F. E., Buhl, E. H., Hormuzdi, S. G., Monyer, H. & Whittington, M. A. (2003) *Proc Natl Acad Sci U S A* **100,** 1370-4.
6. Kepler, T. B., Marder, E. & Abbott, L. F. (1990) *Science* **248,** 83-5.
7. Sherman, A. & Rinzel, J. (1991) *Biophys J* **59,** 547-59.
8. Kopell, N. & Ermentrout, B. (2004) *Proc Natl Acad Sci U S A* **101,** 15482-7.
9. Veruki, M. L. & Hartveit, E. (2002) *J Neurosci* **22,** 10558-66.
10. Rabbah, P., Golowasch, J. & Nadim, F. (2005) *J Neurophysiol*.
11. Hartline, D. K. & Castelfranco, A. M. (2003) *J Comput Neurosci* **14,** 253-69.
12. Hodgkin, A. L. & Huxley, A. F. (1952) *J. Physiol.* **117,** 500-544.
13. Ermentrout, B. (2002) *Simulating, Analyzing, and Animating Dynamical Systems: A Guide to XPPAUT for Researchers and Students* (Soc for Industrial & Applied Math.
14. Rall, W., Segev, I., Rinzel, J. & Shepherd, G. M. (1995) *The theoretical foundation of dendritic function : selected papers of Wilfrid Rall with commentaries* (MIT Press, Cambridge, Mass.).
15. Schmitz, D., Schuchmann, S., Fisahn, A., Draguhn, A., Buhl, E. H., Petrasch-Parwez, E., Dermietzel, R., Heinemann, U. & Traub, R. D. (2001) *Neuron* **31,** 831-40.
16. Deans, M. R., Gibson, J. R., Sellitto, C., Connors, B. W. & Paul, D. L. (2001) *Neuron* **31,** 477-85.
17. Edwards, D. H., Yeh, S. R. & Krasne, F. B. (1998) *Proc Natl Acad Sci U S A* **95,** 7145-50.
18. Tresch, M. C. & Kiehn, O. (2000) *Nat Neurosci* **3,** 593-9.
19. Kopell, N., Abbott, L. F. & Soto-Trevino, C. (1998) *Physica D* **121,** 367-395.
20. Kandler, K. & Katz, L. C. (1998) *J Neurosci* **18,** 1419-27.
21. Hata, Y., Tsumoto, T. & Stryker, M. P. (1999) *Neuron* **22,** 375-81.
22. Konur, S. & Ghosh, A. (2005) *Neuron* **46,** 401-5.
23. Traub, R. D., Kopell, N., Bibbig, A., Buhl, E. H., LeBeau, F. E. & Whittington, M. A. (2001) *J Neurosci* **21,** 9478-86.
24. Beierlein, M., Gibson, J. R. & Connors, B. W. (2000) *Nat Neurosci* **3,** 904-10.
25. Tamas, G., Buhl, E. H., Lorincz, A. & Somogyi, P. (2000) *Nat Neurosci* **3,** 366-71.
26. Lewis, T. J. & Rinzel, J. (2003) *J Comput Neurosci* **14,** 283-309.
27. Chow, C. C. & Kopell, N. (2000) *Neural Comput* **12,** 1643-78.
28. Angstadt, J. D. & Friesen, W. O. (1991) *J Neurophysiol* **66,** 1858-73.
29. Fukuda, T. & Kosaka, T. (2003) *Neuroscience* **120,** 5-20.
30. Pappas, G. D. & Bennett, M. V. (1966) *Ann N Y Acad Sci* **137,** 495-508.

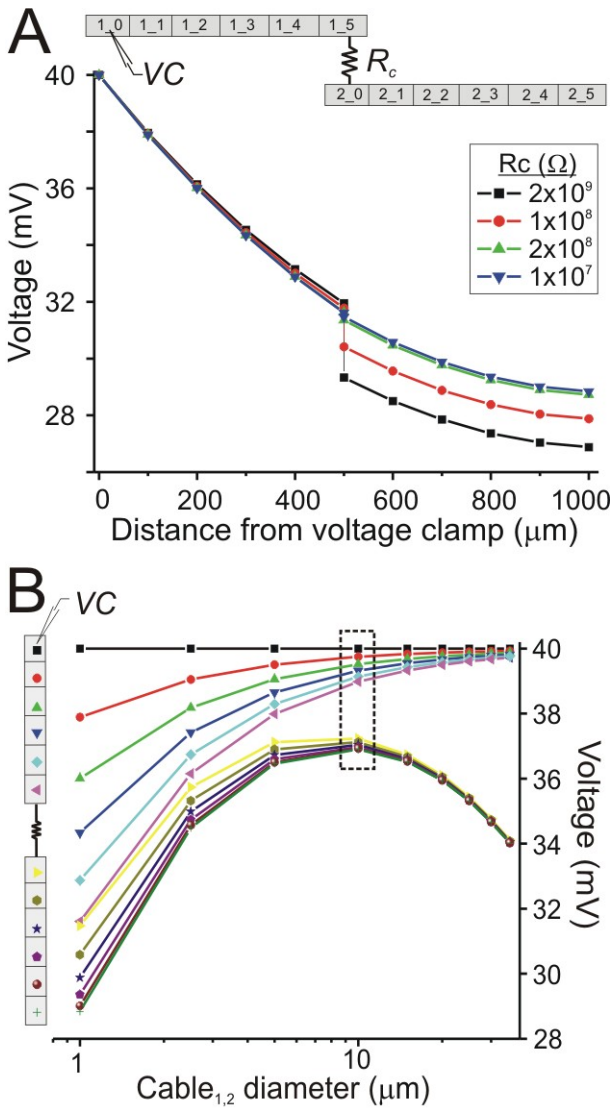

Figure 1. Steady state behavior of a model of two cables coupled by a gap junction. Numerical simulations of voltages along two electrically coupled cables, both with R_m = 40 kΩcm^2, R_i = 60 Ωcm, C_m = 10^{-6}F/cm^2, length = 600 μm. Each cable is divided into 6 isopotential compartments of equal length, and connected at one end by a gap junction of resistance R_c. The voltage of the first compartment of cable 1 (V_{1_0}) was clamped to 40mV. **A.** *Top*: Schematic diagram indicating compartmentalization and coupling of the two cables. *Bottom*: Voltage versus position along both cables. Both cables have diameter 1 μm. **B.** *Left*: Schematic diagram indicating spatial location of voltages shown. R_c = 10^7 Ω. *Right*: The voltage at each position is shown as a function of cable diameter (colored symbols and lines). The diameters of both cables were varied simultaneously.

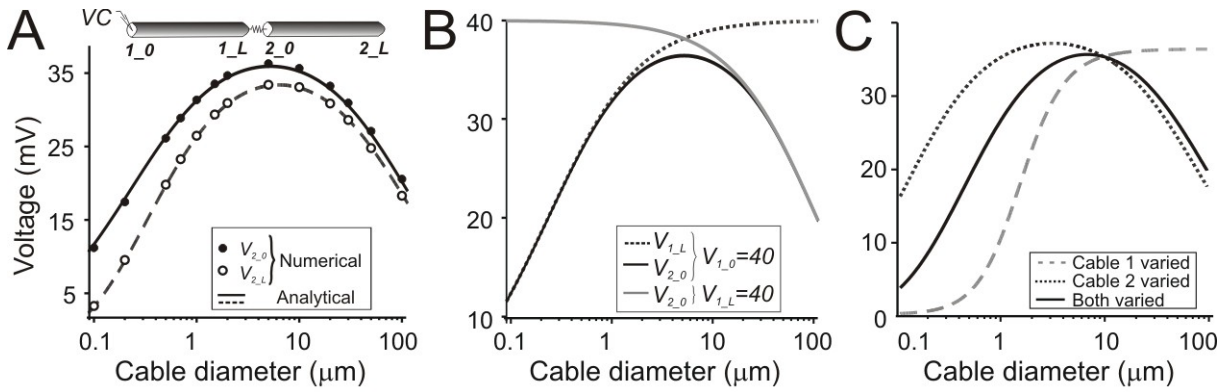

Figure 2. Analytical solutions showing the dependence of voltage spread on cable diameter. **A**. *Top*: Schematic diagram of the two coupled cables. R_c = 2x10^7 Ω, R_m = 40 kΩcm^2, R_i = 60 Ωcm, $l_{1,2}$ = 0.06 cm. *Bottom*: Voltage changes vs. cable diameter for beginning (solid symbols, line) and end of cable 2 (open symbols, dashed line) where calculated numerically (symbols) and analytically (lines, see Methods). Diameters of both cables were varied simultaneously. **B**. Either the beginning (V_{1_0} = 40mV, black lines) or the end of cable 1 was voltage clamped (V_{1_L} = 40mV, grey line) and the voltage at the end of cable 1 (V_{1_L}, dashed line) or beginning of cable 2 (V_{2_0}, solid lines) were calculated analytically and are plotted against the cable diameter. Both cables were varied simultaneously. **C**. Effects of changing the diameter of each cable independently on voltage at the end of cable 2 (broken lines; diameter of fixed cable = 10 μm). For comparison we also show simultaneous diameter variations in both cables (black trace).

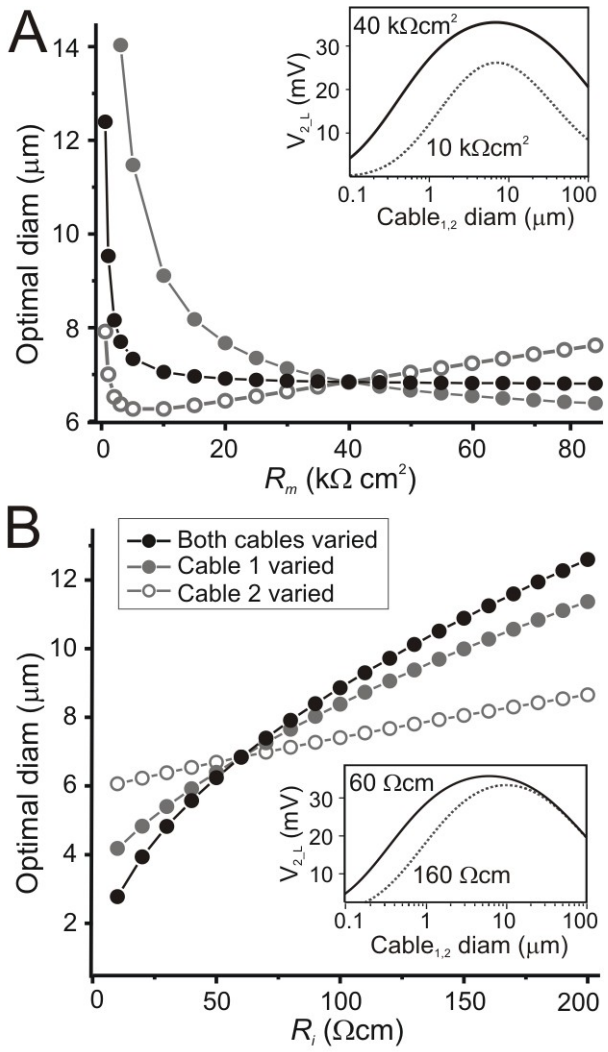

Figure 3. Effect of membrane properties on optimal diameter. Analytical results calculated for two cables of equal length (600 μm) connected by a gap junction of R_c = 2x10^8 Ω. Beginning of cable 1 was clamped to 40mV. **A**. Optimal diameter when R_m values of either only cable 1 (grey filled symbols; R_{m2} = 40 kΩcm^2), only cable 2 (grey open symbols; R_{m1} = 40 kΩcm^2), or both cables were varied simultaneously (black symbols). *Inset*: Steady state diameter tuning curve for two R_m values measured at end of cable 2 (both cable diameters varied simultaneously) show the effect of R_m on attenuation and sharpness of tuning curve. R_i=60 Ωcm. **B**. Optimal diameter when R_i values of either only cable 1 (grey filled symbols; R_{i2} = 60 Ωcm), only cable 2 (grey open symbols; R_{i1} = 60 Ωcm), or both cables were varied simultaneously (black symbols). R_m = 40 kΩcm^2. *Inset*: Steady state diameter tuning curve for two values of R_i measured at end of cable 2 (both cable diameters varied simultaneously) show the effect of R_i on attenuation and sharpness of tuning curve.

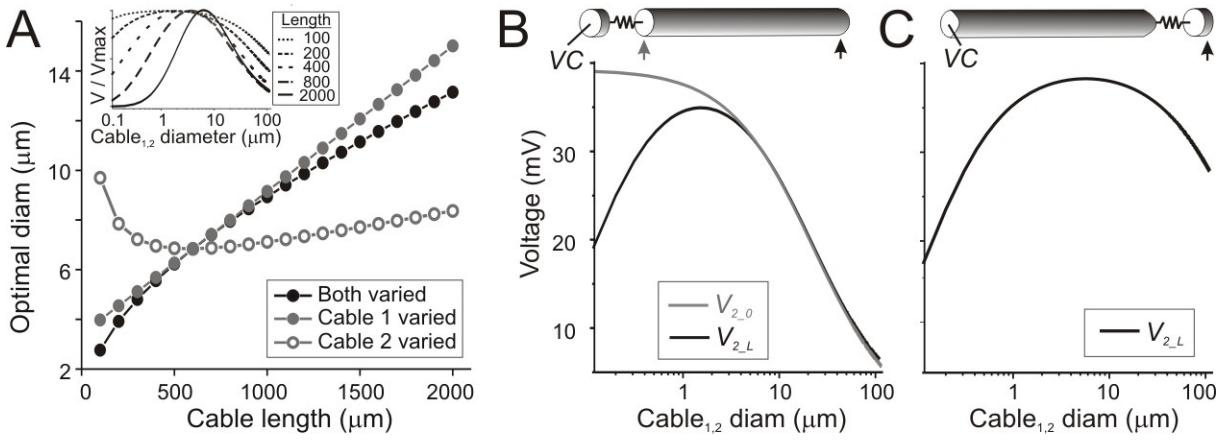

Figure 4. Effect of cable length on optimal diameter. Analytical results were calculated for two cables with varying lengths connected by a gap junction of $R_c = 2x10^7$ Ω. Beginning of cable 1 was clamped to 40mV. **A**. Optimal diameter for varying lengths of either only cable 1 (filled grey symbols; l_2 = 600 μm), only cable 2 (open grey symbols; l_1 = 600 μm), or both cables varied simultaneously (black symbols). R_i = 60 Ωcm; R_m = 40 kΩcm^2. *Inset*: Diameter tuning curves normalized measured at V_{2_L} to their maximum amplitudes for cables of different length (both cables diameters varied simultaneously) to show the shifting of the peak. Not shown is an increased voltage attenuation for increasingly longer cables. **B**. Limit case when cable 1 is isopotential (l_1 = 20 μm; l_2 = 600 μm) showing the diameter tuning curves for V_{2_0} (grey line) and V_{2_L} (black line). **C**. Limit case when cable 2 is isopotential (l_1 = 600 μm; l_2 = 20 μm) showing the diameter tuning curves at the end of cable 2.

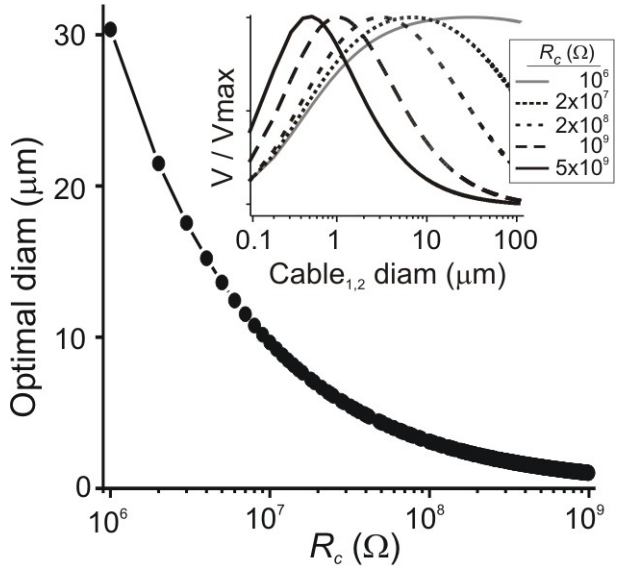

Figure 5. Effect of gap junction resistance R_c on optimal diameter. For both cables R_m = 40 kΩcm^2, R_i = 60 Ωcm, length = 600 μm. Beginning of cable 1 is clamped to 40mV. **A**. Optimal diameter as a function of R_c. *Inset:* Normalized diameter tuning curve at end of cable 2 (V_{2_L}) for 5 different values of R_c to show the shift in optimal diameter and increasing sharpness of this curve with increasing R_c. Not shown is the increasing voltage attenuation as R_c increases.

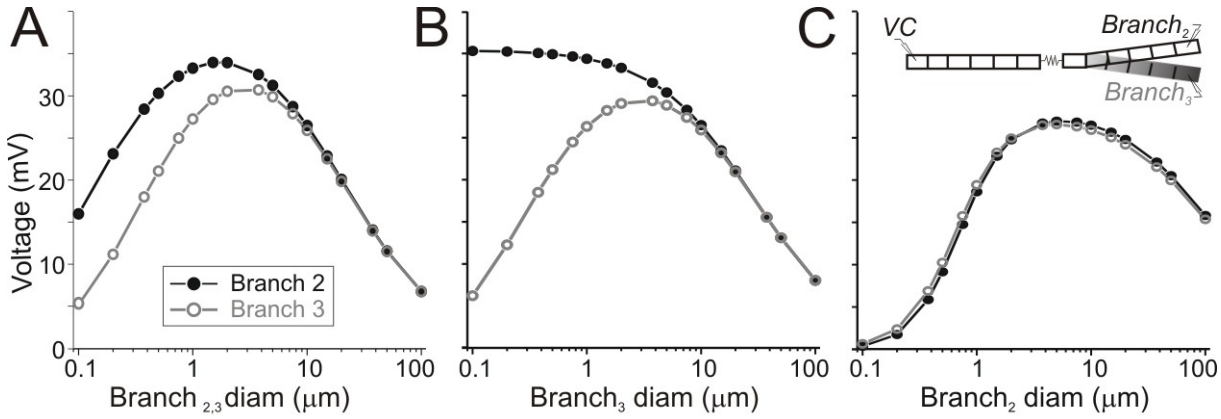

Figure 6. Effect of cable branching on optimal diameter. Numerical simulations performed for model of a primary branch (branch 2) with membrane/cable properties R_{m2} = 40 kΩcm^2, R_{i2} = 60 Ωcm, l_2 = 600 μm connected to a cable of identical properties (cable 1) by a gap junction of resistance $R_c = 2\text{x}10^7$ Ω. A secondary (daughter) branch 3 emerges from the end of the first compartment of branch 2 (schematic diagram in C). The properties of branch 3 are the same as those of branch 2 except that R_{m3} = 10 kΩcm^2. The beginning of cable 1 was voltage clamped at 40mV and its properties, including its diameter, remained fixed. The voltage changes at the tips of both primary (black symbols) and secondary branches (grey symbols) are plotted as a function of branch diameter. **A**. The diameters of both branch 2 and branch 3 are varied simultaneously. **B**. The diameter of branch 2 is fixed at 10 μm and the diameter of branch 3 is varied. **C**. The diameter of the branch 3 is fixed at 10 μm and the diameter of branch 2 is varied.

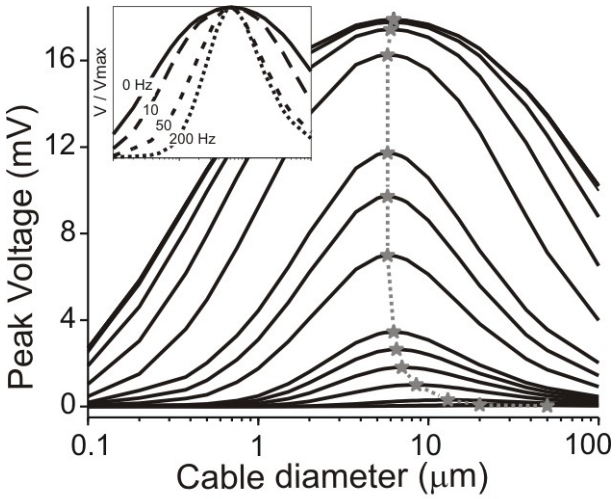

Figure 7. Effect of input frequency on optimal diameter. Two cables of length = 600 μm, R_m = 40 kΩcm^2, R_i = 60 Ωcm, were coupled with a R_c = 2x10^7 Ω. Sinusoidal voltage clamp signals of amplitude 20mV but different frequencies were applied to the beginning of cable 1 and both cable diameters were varied together. Graph shows diameter tuning curve at the end of cable 2 (V_{2_L}). The stars correspond to the optimal diameters for a series of signals of increasing frequencies (top to bottom traces). The vertical dotted line simply connects the stars for added visibility. *Inset*: Diameter tuning curves for 0 Hz (steady state), 10, 50 and 200 Hz normalized to match the peak voltage value observed at steady state (0 Hz) showing the increased sharpness of the curves with increasing input frequency.

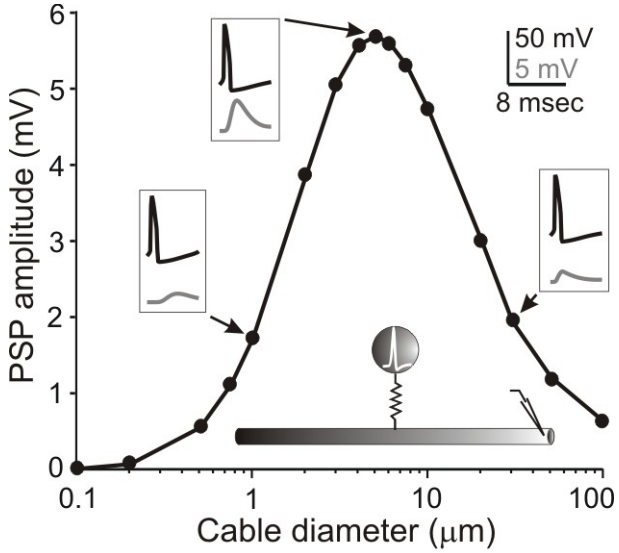

Figure 8. Effect of cable diameter on action potential mediate PSPs across gap junctions. A single-compartment neuron (Methods) capable of producing an action potential is coupled via a gap junction of R_c = 2x10^7 Ω to the center of a passive cable 3100 μm long, R_m = 40 kΩcm^2, R_i = 60 Ωcm. A PSP is measured at one end of the cable for different diameters. Insets show the action potential in cell 1 (black, top trace) and the PSP at the end of the cable (grey, bottom trace) for three different cable diameters .